Model for Fe^{2+} intracenter-induced photoconductivity in InP:Fe

D. C. Look
Physics Department, University of Dayton, Dayton, Ohio 45469
(Received 11 June 1979)

We have observed a broad, room-temperature photoconductivity band, with a peak at 0.44 eV, in Fe-doped InP. This band is attributed to an Fe^{2+} intracenter optical excitation, followed by a thermal excitation to the conduction band. We derive a photoconductivity expression which takes into account optical and thermal transitions between impurity ground and excited states, within the band gap, and the conduction band. The parameters yielded by the model include a thermal excitation prefactor of 1×10^{11} sec^{-1}, an electron capture cross section of 1×10^{-15} cm^2, a spontaneous recombination coefficient of 1×10^{6} sec^{-1}, and an Fe concentration of 2×10^{16} cm^{-3}. The experimental temperature dependence of the photoconductivity is in the right direction, but is smaller than predicted by the model.

I. INTRODUCTION

Iron-doped InP is an important high-resistivity substrate material for InP and GaInAsP devices. The resistivity typically ranges from 10^7 to 10^8 Ωcm, controlled by Fe centers about 0.64–0.68 eV below the conduction band, according to Hall-effect and resistivity measurements.[1-4] The Fe evidently substitutes for In, becoming Fe^{2+} (d^6 configuration) upon accepting an electron from the shallow donors. The atomic ^5D ground-state term breaks into a ^5E ground state and a $^5T_2$ excited state under the influence of the tetrahedral (T_d) crystal field of the zinc-blende lattice. Closely spaced sharp zero-phonon lines, at about 0.35 eV, have been observed at low temperature in photoluminescence[5] and absorption[3,5] spectra, and these lines have been attributed to transitions between the ^5E and $^5T_2$ states. Furthermore, a broad absorption band, peaking at 0.44 eV, has been seen at room temperature.[3,4] (The peak shifts to slightly lower energies at liquid-nitrogen temperature.[3]) In another publication[6] we have described this broad band as resulting from a moderately strong electron-lattice interaction in the $^5T_2$ state, possibly a dynamic Jahn-Teller effect.[7] In this paper we examine the photoconductivity process itself, in particular, how the photoconductivity is related to the absorption. The model used is quite general and should be applicable to other situations in which intracenter transitions within the gap are important to the photoconductivity process. The parameters deduced for InP:Fe are all of reasonable magnitude and yield valuable information about excitation and capture processes. The predicted temperature dependence of the photoconductivity, however, is greater than that actually observed.

II. CONDUCTIVITY DATA

Three InP:Fe samples (designated A, B, and C), from three different manufacturers, form the basis of this study.[8] All three, to our knowledge, were grown by the Czochralski method, and were cut to typical dimensions of $1.0\times0.5\times0.03$ cm. The dark resistivities (ρ_0), presented in Table I, are typical of those observed by workers in other laboratories.[1-4] The carrier concentrations (n_0) and mobilities (μ_{n0}) were determined by a mixed-conductivity analysis[9] and thus are not simply related to the resistivities; i.e., part of the dark conductivity in each case is due to hole conduction, even though the samples have negative (n type) Hall coefficients. (To our knowledge, this is the first report of mixed conductivity measurements in InP.) The temperature dependence of n_0 for sample A is shown in Fig. 1; the other samples showed similar dependences. The calculated thermal activition energy, 0.64 eV, is also typical of those measured by other workers.[1-4]

Photoconductivity (PC) data for samples A–C are presented in Fig. 2. The monochromator was limited to light energies greater than 0.36 eV. In weak signal regions, e.g., near 0.6 eV, ac (20 Hz) measurements were necessary; these were normalized to dc measurements taken in the stronger signal regions. A strong atmospheric absorption band obscured data in a narrow range around 0.45 eV; however, PC spectra observed on another apparatus showed nothing unusual here. Note from Fig. 2 that only Fe-doped samples show the band at 0.44 eV.

Photo-Hall (PH) spectra for sample B are presented in Fig. 3. (The PH spectra for sample A are similar.) Above 0.7 eV, $R\sigma$ begins to increase (i.e., becomes less negative) due to

TABLE I. Dark electrical characteristics of InP samples at 297 °K.

Sample	Manufacturer	ρ_0 (Ω cm)	μ_{n0} $\frac{cm^2}{V sec}$	n_0 (cm^{-3})	$(E_{CB}-E_F)$ (eV)
Fe-doped: A	Metals Research Ltd.	1.7×10^{7}	2.4×10^{3}	1.0×10^{8}	0.565
B	Varian Assoc.	2.9×10^{7}	3.0×10^{3}	4.3×10^{7}	0.587
C	Naval Research Labs.	1.0×10^{7}	3.0×10^{3}	8.6×10^{7}	0.569
Cr-doped	Varian Assoc.	1.5×10^{4}	3.1×10^{3}	1.3×10^{11}	0.382
Undoped	Varian Assoc.	7.5×10^{-1}	4.0×10^{3}	2.1×10^{15}	0.136

greater hole conductivity relative to the electron conductivity. Careful mixed-conductivity measurements[9] show that this increase in $R\sigma$ is mainly due to the onset of a hole excitation, rather than, say, a diminishing electron concentration, or electron mobility. Thus, we can conclude that the observed PC *above* 0.7 eV is primarily due to the interaction of impurity states with the *valence* band (VB), rather than with the conduction band (CB). Below 0.7 eV, the converse is true, as will be shown later. Temperature-dependent PC measurements were carried out at 263, 297, 326, and 362°K, on sample A, and the results are shown in Fig. 4. Data were difficult to obtain at temperatures above and below this range. The Dewar used for these measurements contained Pyrex windows, which strongly absorbed the low-energy light ($h\nu \lesssim 0.45$ eV); thus, data in this energy region contained a high scatter and are not shown in Fig. 4.

III. ABSORPTION AND EMISSION SPECTRA

Four, sharp photoluminescence lines have been observed by Koschel *et al.*[5] near 0.35 eV at low

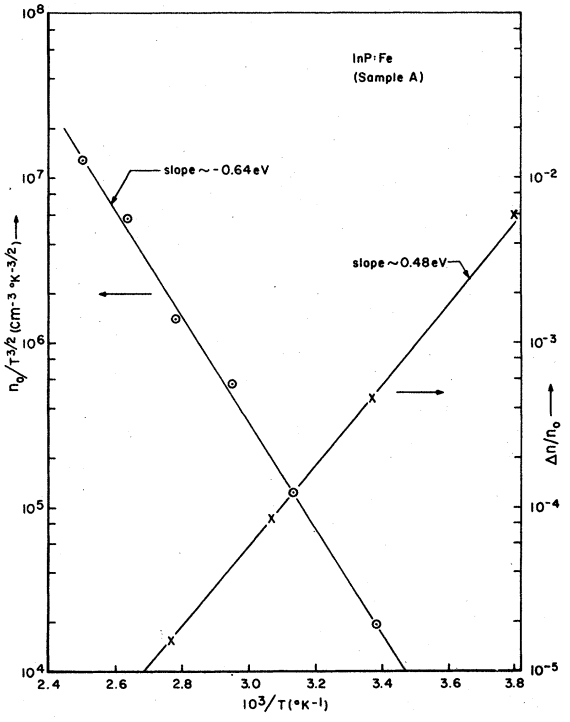

FIG. 1. Arrhenius plots of the dark carrier concentration n_0, and the ratio of the photoexcited carrier concentration Δn, at 0.52 eV, to n_0, for sample A.

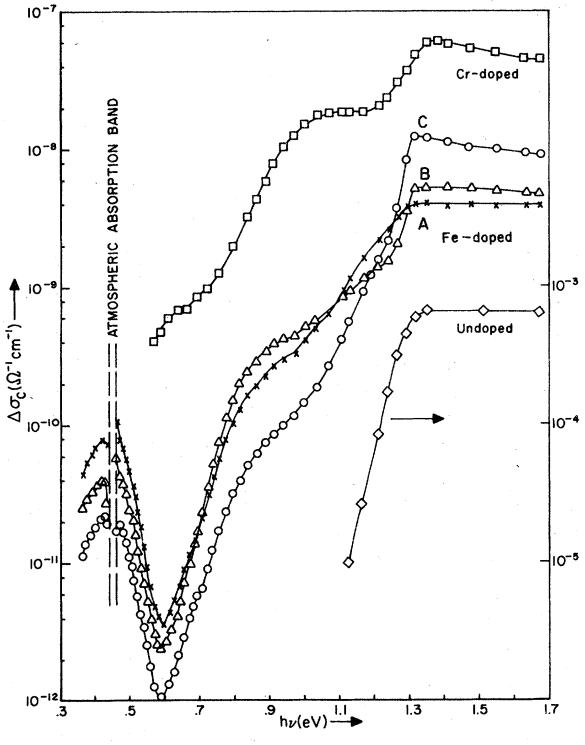

FIG. 2. Spectral dependence of the photoconductivity $\Delta\sigma_c$ for several Fe-doped, Cr-doped, and undoped InP samples. A description of the samples is given in Table I. Note that a strong atmospheric absorption band obscures data near 0.45 eV.

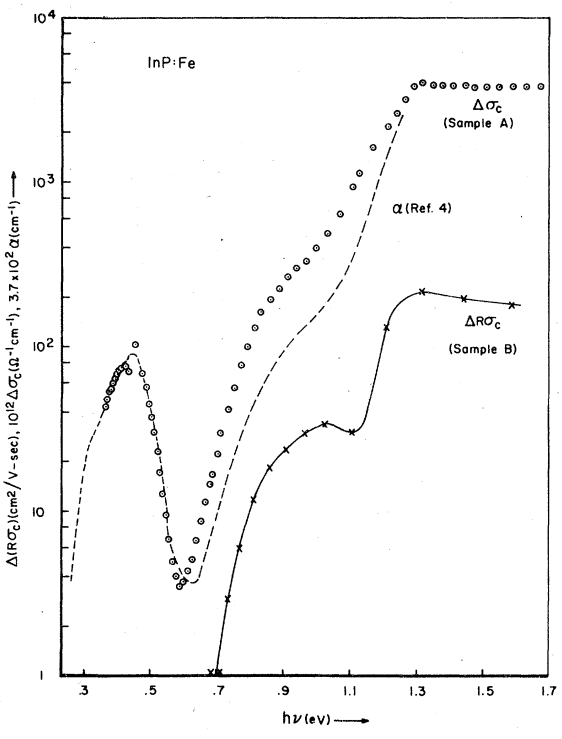

FIG. 3. Spectral dependences of the photoconductivity $\Delta\sigma_c$ for sample A, photo-Hall mobility change $\Delta(R\sigma_c)$ for sample B, and absorption coefficient α for an InP:Fe, Sn sample from Ref. 4. The curves for α and $\Delta\sigma_c$ are normalized to each other at 0.50 eV.

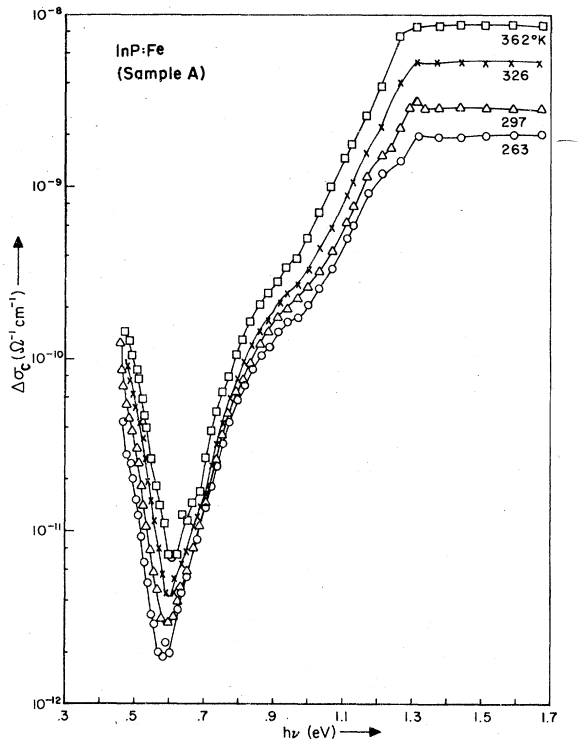

FIG. 4. Spectral dependence of the photoconductivity $\Delta\sigma_c$ for sample A at various temperatures. Below 0.45 eV, the monochromatic light was strongly absorbed by the Pyrex windows of the Dewar.

temperature, and have been explained as zero-phonon lines between the lowest $^5T_2$ state, and four of the five spin-orbit split ^5E states. Sharp absorption lines appear at nearly the same positions.[3,5] An analysis of these spectra[5] suggests that the ^5E ground state is well described by the crystal-field picture, without any significant Jahn-Teller (JT) perturbations; indeed, this also seems to be the case for the Fe^{2+} and Cr^{2+} ^5E states in several of the II-VI compounds which have been studied in detail.[10-12] The $^5T_2$ state, on the other hand, has often been found to exhibit strong JT effects for $d^4(Cr^{2+})$ or $d^6(Fe^{2+})$ configurations in tetrahedral symmetry.[7,10,12] For the Fe^{2+} cases the JT effect is often dynamic, rather than static, and the primary manifestation of this phenomenon is a sharp reduction in the spin-orbit splitting of the $^5T_2$ levels.[7] Thus, the zero-phonon lines are much more closely spaced than the 350–500 cm^{-1} spread which would be expected from spin-orbit splitting in the absence of a JT perturbation.[10] It is quite reasonable that the lack of any observed higher-energy zero-phonon line in InP:Fe^{2+} is also due to a dynamic JT effect. Indeed, a dynamic JT effect has been invoked[13] to explain the absorption spectra in a similar system, GaAs:Fe^{2+}. An additional manifestation of this phenomena would be the existence of a series of vibronic (vibrational-electronic) levels associated with the $^5T_2$ electronic state, and we believe that our 0.44-eV absorption band is due to Franck-Condon transitions from the ^5E state to this set of vibronic levels.[7,14] This model would not preclude the appearance of the 0.35-eV zero-phonon lines, as long as the electron-lattice interaction were not overwhelmingly strong. These ideas are discussed in more detail in a separate publication.[6]

Iseler's 300°K absorption data[4] are presented in Fig. 3, along with our PC data. (The two sets of data are normalized at 0.50 eV.) It is seen that the shapes of the spectra are nearly equivalent, especially in the resonance region. Because of this similarity we do not need to know the details of the $^5T_2$ level structure in order to discuss the photoconductivity; i.e., the PC is simply proportional to the absorption, whatever the cause of the latter.

IV. PHOTOCONDUCTIVITY MODEL

It is convenient to define three spectral regions for the purposes of this study: region 1, the "resonance" region, $0.27 < h\nu < 0.59$ eV; region 2, $0.59 < h\nu < 0.70$ eV; and region 3, $0.70 \lesssim h\nu \lesssim 1.34$ eV (the 297°K band gap). In region 1 we will show that the absorption is due to the optical excitation, ${}^5E \rightarrow {}^5T_2$, and that the photoconductivity involves this transition plus the *thermal* excitation, ${}^5T_2 \rightarrow$ CB. In region 2, both the absorption and PC are due to the optical transition ${}^5E \rightarrow$ CB. In region 3, as discussed earlier, the optical transition VB $\rightarrow {}^5E$ becomes important above 0.70 eV, and then, eventually, VB $\rightarrow$ CB transitions will dominate. Only regions 1 and 2 are of much interest to us here.

To determine the form of the ${}^5T_2 \rightarrow$ CB thermal-excitation terms we first consider a specific ${}^5T_2$ structure, namely, that resulting from the interaction of the ${}^5T_2$ electronic state with vibrational modes of E symmetry. Indeed, this is evidently an important interaction in several of the Fe-doped II-VI compounds,[10] as mentioned earlier, and the vibronic energy-level structure is well known: $\epsilon_n = \epsilon_0' - E_{JT} + (n_1 + n_2 + 1)\hbar\omega$, where E_{JT} is the Jahn-Teller energy and ω is the angular frequency of the vibrational mode. (Further discussion of this problem may be found in Ref. 7.) The ground state of this system has energy $\epsilon_0 = \epsilon_0' - E_{JT} + \hbar\omega$, but eventually, at $n_1 + n_2 = n_{CB}$, the vibronic levels will overlap the conduction band. We assume that electrons excited from ${}^5E$ to ${}^5T_2$ thermalize quickly among the vibronic states and, from a naive point of view, we also assume that those electrons in states with $n > n_{CB}$ are released to the conduction band. Then the photoconductivity will be proportional to

$$1 - \sum_0^{n_{CB}} d_n \exp(-\epsilon_n/kT) \Big/ \sum_0^{\infty} d_n \exp(-\epsilon_n/kT),$$

where d_n is the degeneracy of the nth level. For this system, $d_n = n + 1$, and the result is as follows: the photoconductivity is $\propto \exp(-x - y)\{1 + (x + y)[1 - \exp(-y)]\}$, where $x \equiv E_0/kT$ and $y \equiv \hbar\omega/kT$. (Here, $E_0 \equiv |\epsilon_{CB} - \epsilon_0|$.) The important point here is that the primary temperature dependence is $\exp(-E_0/kT)$, since $E_0 \gg \hbar\omega$ for these deep levels. Somewhat different models, and different approaches to this problem, yield essentially the same result. Thus, from the photoconductivity point of view we need consider only the ${}^5T_2$ ground state, and this approximation greatly simplifies the analysis.

In view of the above discussion the appropriate room-temperature energy diagram should be as shown in Fig. 5. The placement of the ${}^5E$ level

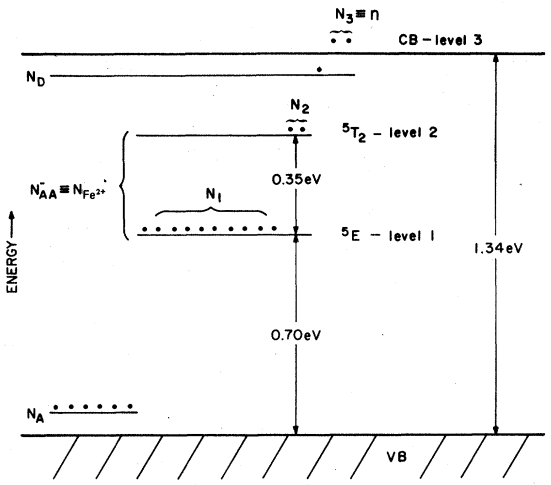

FIG. 5. Proposed room-temperature energy diagram for Fe^{2+} in InP. The various listed quantities are explained in the text, in regard to the derivation of Eq. (6).

has two supporting pieces of evidence: (1) the thermal activation energy, 0.64 eV, which should be $E(\text{CB}) - E({}^5E)$, at least at low temperatures, and (2) the onset of hole excitation at 0.70 eV which should be $E({}^5E) - E(\text{VB})$, at room temperature. Note that $0.64 + 0.70 = 1.34$ eV, the room-temperature band gap. The placement of the ${}^5T_2$ ground state is then given by the energy of the zero-phonon lines observed by Koschel *et al.*[5] and Ippolitova *et al.*[3]; i.e., $E({}^5T_2) - E({}^5E) \simeq 0.35$ eV.

We can depict the transitions rates between the various levels shown in Fig. 5 as follows:

$$W_{12} = I_0\sigma_{p12} + \nu_{12}\exp(-E_{12}/kT), \tag{1a}$$

$$W_{21} = I_0\sigma_{p21} + \nu_{21}\exp(-E_{21}/kT) + B, \tag{1b}$$

$$W_{13} = I_0\sigma_{p13} + \nu_{13}\exp(-E_{13}/kT), \tag{1c}$$

$$W_{31} = v\sigma_{e1}(N_{AA} - N_D + N_D^0 + N_A + n)$$
$$\simeq v\sigma_{e1}(N_{AA} - N_D + N_A), \tag{1d}$$

$$W_{23} = I_0\sigma_{p23} + \nu_{23}\exp(-E_{23}/kT), \tag{1e}$$

$$W_{32} \simeq v\sigma_{e2}(N_{AA} - N_D + N_A), \tag{1f}$$

where W_{ij} is the rate for transitions from level i to level j. Here I_0 is the light intensity (photons/cm^2 sec), σ_{pij} is the cross section for photo-excitation from level i to level j, $\nu_{ij}\exp(-E_{ij}/kT)$ is the thermal transition rate between levels i and j (ν_{ij} should not be confused with ν, the frequency of the impinging light), B is the spontaneous recombination rate from level 2 to level 1, v is the electron velocity, σ_{ei} is the electron capture cross section for the empty level i, and N_{AA}, N_D, and N_A are the deep acceptor (Fe), shallow donor,

and shallow acceptor concentrations, respectively. All energies here are absolute values measured with respect to the CB. Note that we have included no interactions with the VB, and thus Eqs. (1) hold only in regions 1 and 2, as discussed earlier. Note also that the assumed form of the thermal transition rates, $\nu_{ij}\exp(-E_{ij}/kT)$, depends upon the validity of Boltzmann statistics; i.e., $\exp(-E_{ij}/kT)\ll 1$.

The appropriate coupled rate equations that we must solve are

$$\frac{dN_i}{dt} = -N_i \sum_{j\neq i} W_{ij} + \sum_{j\neq i} N_j W_{ij}, \quad i,j = 1,2,3 \tag{2}$$

together with the supplementary condition

$$N_1 + N_2 + N_3 = N_D - N_D^0 - N_A . \tag{3}$$

Here N_1, N_2, and N_D^0 are the concentrations of *occupied* ^5E states, $^5T_2$ states, and shallow donor states, respectively, as depicted in Fig. 5; also $N_3 \equiv n$, the free electron concentration. In semi-insulating material, such as InP:Fe, the condition $n, N_D^0 \ll N_D, N_A, N_{AA}$ will hold. At steady state, $dN_i/dt = 0$ and we can solve Eqs. (2) and (3) to yield

$$n \equiv N_3 = \frac{N_D - N_A}{1 + B/A}, \tag{4}$$

where

$$A = W_{13}W_{21} + W_{23}(W_{13} + W_{12}), \tag{5a}$$

$$B = (W_{31} + W_{32})(W_{21} + W_{12}) + W_{31}W_{23} + W_{32}W_{13} . \tag{5b}$$

Equation (4) is simplified somewhat for semi-insulating samples because $B/A \gg 1$, except at very high temperatures. However, it is obvious from Eqs. (1) and (5) that there are still a great many terms involved in Eq. (4). The magnitudes of these terms, relative to each other, are to a large extent controlled by the $\exp(-E_{ij}/kT)$ factors, where the E_{ij}'s are given in Fig. 5. By comparing all the terms, and dropping the small ones, we can arrive at the following expression for the photoexcited electron concentration $\Delta n \equiv n(I_0) - n(0)$:

$$\Delta n = \frac{1}{N_{AA}/(N_D - N_A) - 1}\left[I_0\left(\frac{\sigma_{p12}\nu_{23}\exp(-E_{23}/kT)}{v(\sigma_{e1}+\sigma_{e2})B}F_1(T) + \frac{\sigma_{p13}}{v(\sigma_{e1}+\sigma_{e2})}F_2(T)\right) + I_0^2\frac{\sigma_{p12}(\sigma_{p13}+\sigma_{p23}) + \sigma_{p13}\sigma_{p23}}{v(\sigma_{e1}+\sigma_{e2})B}F_3(T)\right], \tag{6}$$

$$n_0 \equiv n(I_0 = 0) = \frac{1}{N_{AA}/(N_D - N_A) - 1}\frac{(\nu_{13}B + \nu_{12}\nu_{23})\exp(-E_{13}/kT)}{v(\sigma_{e1}+\sigma_{e2})B}F_3(T)F_4(T), \tag{7}$$

where

$$F_1(T) = \frac{\nu_{13}B + \nu_{12}\nu_{23} + \nu_{13}\nu_{23}\exp(-E_{23}/kT)}{\nu_{13}B + \nu_{12}\nu_{23} + \nu_{13}\nu_{23}[(2\sigma_{e1}+\sigma_{e2})/(\sigma_{e1}+\sigma_{e2})]\exp(-E_{23}/kT)}, \tag{8a}$$

$$F_2(T) = F_1(T)\frac{B(\sigma_{e1}+\sigma_{e2}) + \nu_{23}(2\sigma_{e1}+\sigma_{e2})\exp(-E_{23}/kT)}{B(\sigma_{e1}+\sigma_{e2}) + \nu_{23}\sigma_{e1}\exp(-E_{23}/kT)}, \tag{8b}$$

$$F_3(T) = \left(1 + \frac{\nu_{23}\sigma_{e1}\exp(-E_{23}/kT)}{B(\sigma_{e1}+\sigma_{e2})}\right)^{-1}, \tag{8c}$$

$$F_4(T) = \left(1 + \frac{\nu_{13}\nu_{23}\exp(-E_{23}/kT)}{\nu_{13}B + \nu_{12}\nu_{23}}\right). \tag{8d}$$

It is quite obvious that at low enough temperatures, $F_i(T) \simeq 1, i = 1\text{–}4$. [A reasonable criterion for this is $\nu_{23}B^{-1}\exp(-E_{23}/kT) \ll 1$.] Furthermore, the I_0^2 term is small at typical light intensities; this is verified by the experimental relationship $\Delta n \propto I_0$ in regions 1 and 2. We thus, to a first approximation, can analyze our data by using the first two terms of Eq. (6), with $F_i(T) \simeq 1$, $i = 1, 2$. The first term, which describes region 1, corresponds to an optical excitation from level 1(^5E) to level 2($^5T_2$), and a thermal excitation from level 2 to level 3 (CB). The second term, which is dominant in region 2, involves a direct optical excitation from level 1 to the CB. The third term, which is too small to be observed, involves two optical excitations. Note that Eq. (6) predicts that $\Delta n \propto \sigma_{p12}$ in region 1, and $\Delta n \propto \sigma_{p13}$ in region 2; these relationships are verified in Fig. 3, since Iseler's absorption data[4] are a direct measurement of σ_{p12} and σ_{p13}.

One further point regarding Eq. (6) must be considered, and that is the fact that we really don't measure Δn, but instead $\Delta\sigma_c$, the photoconductivity. However, $\Delta n = \Delta\sigma_c/e\mu_{n0}$, if the electron mobility is not significantly affected by the light; this should be true in regions 1 and 2, in which the photoconductivity is at least three orders of magnitude lower than the dark conductivity. The μ_{n0} for sample A is given in Table I.

V. RESULTS

For region 2, we can combine the second term of Eq. (6) with Eq. (7) to yield

$$\nu_{13}+\nu_{23} \simeq \frac{n_0 I_0 \sigma_{p13}}{\Delta n \exp(-E_{13}/kT)}, \quad \text{(region 2)}. \tag{9}$$

Here we have assumed that $\nu_{12} \simeq B$, in Eq. (6), a condition which holds for a simple two-level system,[15] and which should at least approximately hold in our system. Also, we have let $F_i(T)=1$, $i=1-4$, and will check the validity of this assumption later. For our experiment, $I_0 \simeq 1\times10^{15}$ photons/cm^2 sec, and, for sample A, n_0, $\sigma_{p13}/\Delta n$, and E_{13} may be obtained from Table I, Fig. 3, and Fig. 1, respectively. The result is $\nu_{13}+\nu_{23} \simeq 1\times10^{11}$ sec^{-1}.

Next, by comparing the n_0 in Eq. (7) with that obtained by the usual Fermi-level analysis,[16] we can set

$$\sigma_{e1}+\sigma_{e2} \simeq (\nu_{13}+\nu_{23})/vN_c g_{AA}, \tag{10}$$

where N_c is the conduction-band density of states, and g_{AA} is an effective degeneracy factor. For InP, $N_c \simeq 4.3\times10^{17}$ cm^{-3} at room temperature, and $v \simeq (8kT/\pi m_e^*)^{1/2} \simeq 4.1\times10^7$ cm/sec. The value of g_{AA} is unknown, but for lack of better information we can assume $g_{AA} \simeq 4$, the usual shallow acceptor value.[17] Then Eq. (10) gives $\sigma_{e1}+\sigma_{e2} \simeq 1\times10^{-15}$ cm^2, and, from Eq. (7), $N_{AA}/(N_D-N_A) \simeq 1.2$. This value of the electron-capture cross section is reasonable for a neutral center (Fe^{3+}).[18]

Since our samples were very thin, it was difficult to measure the absorption constant accurately. However, a rough measurement on sample A gave $\alpha \simeq 0.1$ cm^{-1} at the peak. By noting that $\alpha = N_1\sigma_{p12} \simeq N_{\bar{A}A}\sigma_{p12} \simeq (N_D-N_A)\sigma_{p12}$, we can use the σ_{p12} data in Fig. 3 to calculate $N_D-N_A \simeq 2\times10^{16}$ cm^{-3}, and therefore $N_{AA} \equiv N_{Fe} = 1.2(N_D-N_A) \simeq 2.4\times10^{16}$ cm^{-3}. It is interesting that spark-source mass spectrographic (SSMS) measurements on a sample with nearly identical PC characteristics to those of sample A gave $N_{Fe} \simeq 3\times10^{16}$ cm^{-3}.

Finally, in region 1, we can combine Eq. (7) and the first term of Eq. (6) to obtain

$$\frac{\nu_{23}\exp(-E_{23}/kT)}{B} \simeq \frac{\Delta n(\nu_{13}+\nu_{23})\exp(-E_{13}/kT)}{n_0 I_0 \sigma_{p12}} \simeq 0.5 \quad \text{(region 1)}, \tag{11}$$

where $\Delta n/\sigma_{p12}$ is obtained from Fig. 3. [Actually, the left-hand side of Eq. (11) may be obtained directly from the ratio of the first and second terms of Eq. (6).] As discussed before, Eqs. (6) and (7) are valid only in the limit $\nu_{23}B^{-1}\exp(-E_{23}/kT) \ll 1$, and from Eq. (11) it is seen that this criterion is only weakly satisfied. However, an examination of the correction factors, given by Eqs. 8(a)–8(d), shows that, in any case, the $F_i(T)$ are not much different from unity as long as $\nu_{13} \sim \nu_{23}$, $\sigma_{e1} \sim \sigma_{e2}$, and $\nu_{12} \sim B$.

If $\nu_{13} \simeq \nu_{23}$, we can obtain $\nu_{23} \simeq 5\times10^{10}$ sec^{-1} from Eq. (9). Also, from the diagram in Fig. 5 we expect that $E_{23} \simeq 0.29$ eV, and therefore, from Eq. (11), $B \simeq 1\times10^6$ sec^{-1}. If τ_{21} is dominated by the radiative process, it can be shown that the expected oscillator strength will be approximately given[19] by $f_{12} \simeq 2.4\times10^{-9}\tau_{21}^{-1} \simeq 2.4\times10^{-9}B \simeq 3\times10^{-3}$. This value of f_{12} compares favorably with values for Fe^{2+} and Cr^{2+} in several of the II-VI compounds ($f \simeq 5\times10^{-4}$),[10,12] and with the value for Cr^{2+} in GaAs ($f \simeq 3\times10^{-3}$).[20] It should be cautioned here that we have not really *measured* f_{12}, but only determined an approximate value by a very indirect method.

A final check on the model is a measurement of the temperature dependence of Δn. To eliminate the temperature dependences of v and σ_e it is best to use Eq. (11), since the temperature dependence of n_0 is known (cf. Fig. 1). Then, if all of the other parameters in Eq. (11) are temperature independent, we expect that $\Delta n/n_0 \propto \exp[(E_{13}-E_{23})/kT] \simeq \exp(0.35\ \text{eV}/kT)$. However, as seen in Fig. 1, we actually measure $\Delta n/n_0 \propto \exp(0.48\ \text{eV}/kT)$, or $\Delta n \propto \exp(-0.16\ \text{eV}/kT)$, since $n_0 \propto \exp(-0.64\ \text{eV}/kT)$. Thus, Δn is not nearly as temperature dependent as we would have expected it to be. Part of this difference is due to a temperature dependence of σ_{p12}, as discussed elsewhere,[6] and as observed by Ippolitova *et al.*[3]; however, the σ_{p12} dependence is weak in comparison with the Δn dependence. Another possibility involves the correction factors, Eqs. 8(a)–8(d), which, indeed, are temperature dependent and which may be more significant than we have assumed. A third possibility could be experimental error. It is encouraging, though, that the PC temperature dependence is at least in the right direction.

Thus, our model appears to be basically adequate to explain the photoconductivity in InP:Fe.

The calculated excitation and capture parameters are quite reasonable and the calculated Fe concentration agrees well with SSMS measurements. The temperature dependence of the photoconductivity is in the right direction, but is weaker than predicted; this effect should be investigated further.

VI. SUMMARY

We have presented a photoconductivity model applicable to a semiconductor containing deep impurity centers with ground and excited states within the band gap. The model has been applied to Fe^{2+} in InP with reasonable success in fitting the values of the various parameters. The photoconductivity line shape is very similar to the absorption line shape, measured by others, and the line broadening is well described by a model in which the $^5T_2$ state interacts strongly with a lattice mode.[6] The temperature dependence of the photoconductivity, however, is weaker than expected from our model. The reasons for this are not clear, but it may be that the actual picture is more complex than the one we have dealt with here.

ACKNOWLEDGMENTS

We are grateful to E. Swiggard of Naval Research Labs and G. Antypas of Varian for supplying InP:Fe samples grown in their laboratories, and to Y. S. Park for supplying an InP:Fe sample grown by Metals Research Ltd. We are also indebted to D. Walters for carrying out spark-source mass spectrographic measurements on several of these samples. Finally, thanks are due M. Kreitman for some photoconductivity measurements in vacuum. This work was performed at Avionics Laboratory, Wright Patterson Air Force Base, under Contract No. F33615-76-C-1207.

[1]O. Mizuno and H. Watanabe, Electron. Lett. 11, 118 (1975).
[2]K. P. Pande and G. G. Roberts, J. Phys. C 9, 2899 (1976).
[3]G. K. Ippolitova, E. M. Omelyanovskii, N. M. Pavlov, A. Ya. Nashelskii, and S. U. Yakobsen, Sov. Phys. Semicond. 11, 773 (1977).
[4]G. W. Iseler, in *Gallium Arsenide and Related Compounds*, 1978, edited by C. M. Wolfe (Institute of Physics, London, 1979), p. 144.
[5]W. H. Koschel, U. Kaufmann, and S. G. Bishop, Solid State Commun. 21, 1069 (1977).
[6]D. C. Look, Solid State Commun. (to be published).
[7]F. S. Ham, Phys. Rev. 138, A1727 (1965).
[8]Sample A, Metals Research Ltd.; sample B, Varian Assoc.; and sample C, Naval Research Labs.
[9]D. C. Look, J. Phys. Chem. Solids 26, 1311 (1975).
[10]G. A. Slack, F. S. Ham, and R. M. Chrenko, Phys. Rev. 152, 376 (1966).
[11]G. A. Slack and B. M. O'Meara, Phys. Rev. 163, 335 (1967).
[12]J. T. Vallin, G. A. Slack, S. Roberts, and A. E. Hughes, Phys. Rev. B 2, 4313 (1970).
[13]G. K. Ippolitova and E. M. Omelyanovskii, Sov. Phys. Semicond. 9, 156 (1975).
[14]M. D. Sturge, in *Solid State Physics*, edited by F. Seitz, D. Turnbull, and H. Ehrenreich (Academic, New York, 1967), Vol. 20, p. 91. A simplified picture of the absorption process that we are describing may be found in Fig. 30, p. 179, of this reference.
[15]See, e.g., J. I. Pankove, *Optical Processes in Semiconductors* (Dover, New York, 1971), Chap. 9. Equation 9–10 is relevant to our discussion.
[16]See, e.g., R. H. Bube, *Photoconductivity in Solids* (Wiley, New York, 1960), p. 51. A similar relationship to our Eq. (10) is expressed in Bube's Eq. 2.7–17.
[17]W. Kohn, Solid State Phys. 5, 257 (1957).
[18]Reference 16, p. 61.
[19]See, e.g., D. L. Dexter, in *Solid State Physics*, edited by F. Seitz, D. Turnbull, and H. Ehrenreich (Academic, New York, 1958), Vol. 6, p. 353.
[20]G. K. Ippolitova, E. M. Omelyanovskii, and I. Ya. Pervova, Sov. Phys. Semicond. 9, 864 (1976).